

## One picture says it all—high-pressure cells for neutron Laue diffraction on VIVALDI

This article has been downloaded from IOPscience. Please scroll down to see the full text article.

2005 J. Phys.: Condens. Matter 17 S3017

(<http://iopscience.iop.org/0953-8984/17/40/004>)

View [the table of contents for this issue](#), or go to the [journal homepage](#) for more

Download details:

IP Address: 129.252.86.83

The article was downloaded on 28/05/2010 at 06:00

Please note that [terms and conditions apply](#).

# One picture says it all—high-pressure cells for neutron Laue diffraction on VIVALDI

G J McIntyre<sup>1</sup>, L Mélési<sup>1</sup>, M Guthrie<sup>2</sup>, C A Tulk<sup>3</sup>, J Xu<sup>4</sup> and J B Parise<sup>5,6</sup>

<sup>1</sup> Institut Laue-Langevin, BP156, 38042 Grenoble Cedex 9, France

<sup>2</sup> CSEC, School of Physics, University of Edinburgh, Edinburgh EH9 3JZ, UK

<sup>3</sup> Oak Ridge National Laboratory, PO Box 2008, Oak Ridge, TN 37831, USA

<sup>4</sup> Geophysical Laboratory, Carnegie Institute of Washington, 5251 Broad Branch Rd, NW, Washington, DC 20015, USA

<sup>5</sup> Department of Geosciences, State University of New York, Stony Brook, NY 11749-2100, USA

<sup>6</sup> Department of Chemistry, State University of New York, Stony Brook, NY 11749-2100, USA

Received 8 July 2005

Published 23 September 2005

Online at [stacks.iop.org/JPhysCM/17/S3017](http://stacks.iop.org/JPhysCM/17/S3017)

## Abstract

Possible applications of the neutron single-crystal Laue diffraction technique with a large image-plate detector to high-pressure studies are examined. One opposed-piston cell with a Ti–Zr casing is shown to be acceptable for medium pressures. For higher pressures a moissanite-anvil cell with reasonably large accessibility is shown to offer impressive gains in data collection rate as compared to the monochromatic technique. Moreover, the projected forms of the reflections from the sample and anvils facilitate alignment, and the wide wavelength band of the Laue technique allows recovery of reflections masked by the cell pillars, simply by rotation of the cell.

## 1. Introduction

Neutron Laue diffraction with image-plate detection on a thermal beam has proven to be a high-performance technique well suited to small crystals, rapid chemical crystallography, reciprocal-space surveys, and studies of structural and magnetic phase transitions. In its first years of operation at the ILL, VIVALDI (Very-Intense Vertical-Axis Laue Diffractometer; Wilkinson *et al* 2002) has produced spectacular diffraction patterns and exciting new science at a furious rate, with gains in data collection rate over conventional diffractometers of up to a hundredfold. In just a few hours it has produced detailed atomic structural information on small crystals of large organic molecules (e.g. Bau *et al* 2004, Boss *et al* 2004), revealed new magnetic structures (e.g. Schobinger-Papamantellos *et al* 2004), and shown 2D magnetic ordering in astounding clarity (Chung *et al* 2004). Can the advantages of the large-solid-angle Laue technique also be realized in high-pressure crystallography?

After a brief general description of the technique as implemented on VIVALDI we discuss the particular constraints imposed by the technique on high-pressure cells. We then present

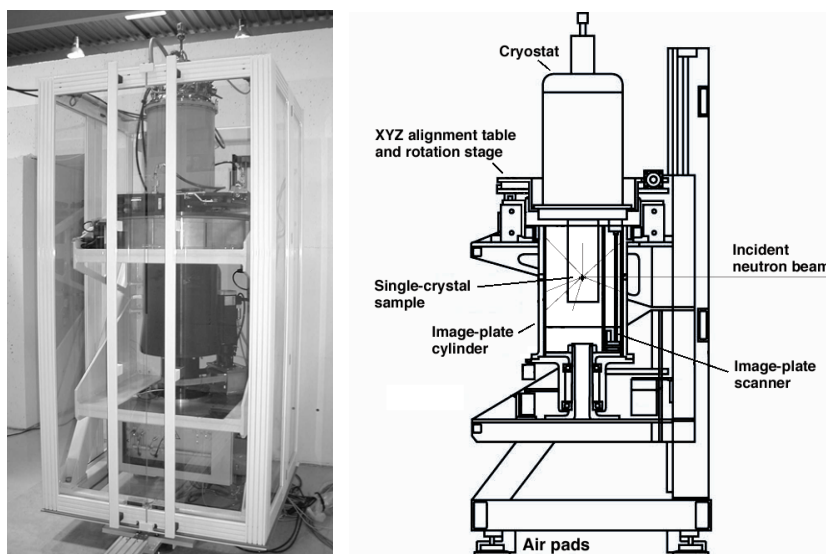


**Figure 1.** The neutron Laue diffractometer, VIVALDI. The sample, located in the middle of the image-plate detector, is bathed in the un-monochromated incident thermal-neutron beam.

early results from two types of existing cells, an opposed-piston cell and an anvil cell, and suggest some design parameters of an optimized cell for single-crystal Laue diffraction.

## 2. VIVALDI

VIVALDI (figure 1) is a cylindrical Laue camera located at the end of an un-monochromated thermal-neutron guide. The camera or detector consists of neutron-sensitive image plates upon which the diffraction pattern from a stationary crystal is recorded. At the end of each exposure the recorded pattern is read out in phonographic mode by rotating the detector while translating a stimulating laser and photomultiplier detector along the length of the cylinder. Both VIVALDI and its sister instrument LADI (Cipriani *et al* 1996), which is used on a cold-neutron beam for macromolecular crystallography, were constructed in close collaboration with the EMBL Grenoble Outstation.

Image plates offer high spatial resolution, good homogeneity, a large dynamical range, extended linearity and no dead-time. The neutron-sensitive image plates are based on the same storage phosphor (BaFBr doped with  $\text{Eu}^{2+}$  ions) used for x-ray image plates, but with  $\text{Gd}_2\text{O}_3$  added; the Gd nuclei act as neutron scintillators by creating a cascade of  $\gamma$ -rays and conversion electrons. For a good-quality crystal the small divergence of the incident beam and the small point-spread function ( $\sim 150 \mu\text{m}$ ) of the detector and read-out system yield Bragg reflections which are barely larger than the projected form of the crystal onto the image plate irrespective of the intensity of the reflection. This allows fine resolution of small weak reflections from nearby strong reflections.

The Laue experiment is itself very simple, entailing collection of one to ten diffraction patterns, successive patterns being distinguished by a rotation of typically  $20^\circ$  or  $30^\circ$  of the crystal about the detector axis. Most data can be displayed, indexed, integrated and scaled to a common wavelength using interactive programs of the CCP4 Laue suite (Helliwell *et al* 1989). The simple geometry, which is usually cylindrically symmetric even for the sample

environment, facilitates correction for absorption, although proper account must be taken of the wavelength dependence.

### 3. Constraints on pressure experiments

Unlike the powder experiment, the single-crystal Laue experiment (whether white-beam or time-resolved) still requires wide access, or many settings (which would eliminate the advantage over the monochromatic technique). The VIVALDI detector subtends  $288^\circ$  in the equatorial plane and  $\pm 52^\circ$  out of the plane. Can a similar solid angle of accessibility be provided by a pressure cell?

Any material in the beam can contribute to background in the diffraction pattern. If the material is truly polycrystalline the additional background will vary slowly across the pattern. If single crystalline it will give a diffraction pattern which we must allow for in integration of the sample pattern. Worst of all, though, is a coarsely polycrystalline material which gives rise to a manifold of single-crystal patterns, and usually renders the measurement unusable. Even common neutron absorbers can increase the background, since the image plates are sensitive to  $\gamma$ -rays, particularly those with energies below 200 keV (Popov and McIntyre 2005).

The broad band of wavelengths means that only ratios of the linear cell dimensions can be determined. Therefore the pressure cannot be determined by including a standard calibrant, such as NaCl, in the sample space. Some other method must be used.

The sample should preferably be mounted with all symmetry axes at angles greater than  $20^\circ$  to the crystal-rotation axis to minimize the number of unique reflections missed. This might be difficult to achieve in the restricted sample space of a pressure cell.

### 4. Possible solutions

Cells with  $360^\circ$  of access horizontally and a large angle vertically require an outer casing that is strong enough—which usually means thick enough—to maintain the applied pressure. Repeated cycling of pressure and temperature may lead to preferred orientation or even growth of single crystals in the casing. The contribution from scattering in the casing to the pattern may be considerable, even if reasonably flat (see figure 2).

Alternatively the casing could consist of just two or three thick pillars separated by large open angles. The region of reciprocal space that is blind at any one setting is the same with an even or with an odd number of pillars of the same total subtended angle. There is however much less freedom in setting angles with an odd number since both blocking of the incident beam and blocking of the transmitted beam must be avoided. An even number of symmetrically spaced pillars is the best choice.

A large vertical angle is easy to achieve at medium pressures (up to 1 GPa) in an opposed-piston cell, and narrow cone-angle anvils could conceivably be considered for medium pressures in an anvil cell. At higher pressures the vertical angle of access must decrease. Nevertheless, present anvil cells that can reach 50 GPa do offer up to  $\pm 50^\circ$  of access vertically (Goncharenko 2004, Xu *et al* 2002), considerably more than the  $\pm 5^\circ$  of a typical 3–4 GPa McWhan-type opposed-piston cell (McWhan *et al* 1979).

Direct measurement of the pressure is possible using a Manganin resistance pressure gauge if space permits or by ruby fluorescence (Mao *et al* 1986, Kernavainis *et al* 2004).

The sample remains stationary during the acquisition of each diffraction pattern. Except for a highly absorbing sample, it is not necessary that the whole sample be bathed in the beam, nor that the aperture be larger than the sample to allow for divergence of the incident beam. Separate scale factors are derived for each pattern in the wavelength normalization. An

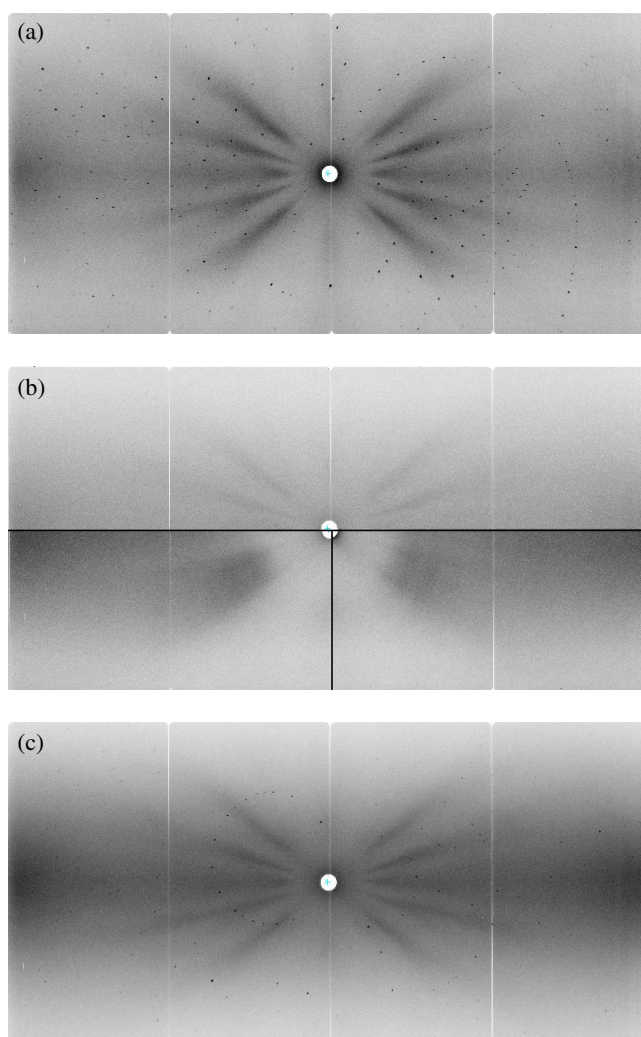


**Figure 2.** Scattering observed on the VIVALDI image-plate detector from various empty and loaded 1 GPa ILL opposed-piston pressure cells: (a) Laue diffraction pattern from a  $3.5 \text{ mm}^3$  crystal of  $(\text{NH}_4)_2\text{Cr}(\text{SO}_4)_2 \cdot 6\text{H}_2\text{O}$  alone; (b) composite image of the scattering from the empty pressure cells: the upper half is for the Ti–Zr cell, 6 mm wall thickness; lower left is for the Cu–Be cell, 4 mm wall thickness; lower right is for the steel cell, 2.5 mm wall thickness; (c) Laue diffraction pattern from the  $(\text{NH}_4)_2\text{Cr}(\text{SO}_4)_2 \cdot 6\text{H}_2\text{O}$  crystal in the Ti–Zr cell. Incident-beam aperture diameter, 4 mm; exposure times: 2 h for (a), 1/2 h for each pattern in (b), 3 h for (c). Each pattern subtends  $244^\circ$  horizontally and  $104^\circ$  vertically; the transmitted beam exits the detector through the hole in the centre. The streaks radiating from the centre and common to all patterns are due to preferred orientation in the aluminium tails of the cryostat.

aperture slightly smaller than the cross-section of the sample can therefore be used to reduce the background from the pressure-cell walls and anvils.

### 5. Trials with medium-pressure opposed-piston cells

During a study of the temperature dependence of the Cr–O bond lengths in Cr ammonium Tutton’s salt (Dobe *et al* 2004), an attempt was made to repeat part of the experiment at a

pressure of 0.5 GPa in an opposed-piston pressure cell. Several cells with different casing materials were at our disposal: Ti–Zr (wall 6 mm thick<sup>7</sup>), Cu–Be (wall 4 mm thick), and maraging steel (wall 2.5 mm thick) (Gobrecht *et al* 1992). Ti–Zr gives negligible coherent scattering, but considerable incoherent scattering. All three cells offer 360° of access in the equatorial plane and  $\pm 48^\circ$  out of the plane.

Figure 2 shows the diffraction pattern from the sample alone, the scattering from the three cells with no sample, and the diffraction pattern from the sample inside the Ti–Zr cell at 1 bar. All measurements were at 300 K inside the VIVALDI He cryostat for which the total thickness of the AG3 and A5 Al heat shields is 4 mm. The incident beam was defined by a 4 mm diameter LiF aperture.

The scattering from the Cu–Be and the steel cells has considerable structure, especially near the scattering from the aluminium cryostat heat shields. Ti–Zr gives the lowest, most nearly uniform background, but higher background at low angles than Cu–Be or steel due to incoherent scattering. The pattern with the sample in the Ti–Zr cell gave integrated intensities 50% lower than those for the sample outside the cell due to absorption in the cell walls, and with an average  $I/\sigma(I)$  25% lower, consistent with the drop in intensity. The slightly higher background had an insignificant effect on the statistics.

In the end, this sensitive sample decomposed before the desired experiment could be performed, but these preliminary observations do show that an opposed-piston cell with a Ti–Zr casing is acceptable for medium pressures.

## 6. A trial with a moissanite-anvil cell

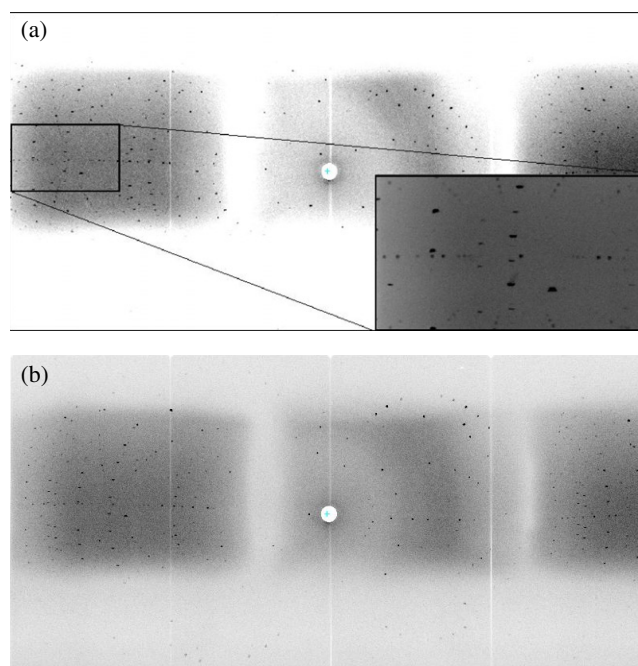
The opportunity arose to test a ‘panoramic’ moissanite-anvil cell from the Geophysical Laboratory (Xu *et al* 2002) for a few hours. The cell contained a  $1 \times 1 \times 0.5 \text{ mm}^3$  crystal of natrolite at 1 bar surrounded by a 1 mm high steel gasket with a 3.5 mm thick wall. The outer steel support has three equally spaced Cd-clad pillars, each of which subtends  $20^\circ$  at the sample, and the vertical access for this test was asymmetric at  $+35^\circ$  and  $-19^\circ$ . (The access would be symmetric at  $\pm 34^\circ$  if the sample was at the centre of the cell.)

Figure 3 shows two diffraction patterns taken with the incident beam defined by a 3.2 mm diameter LiF aperture 17.5 cm from the sample, successive patterns being distinguished by a rotation of  $10^\circ$  in  $\phi$ . The angles were chosen to avoid placing any of the pillars in the direct or transmitted beams. A tapered B<sub>4</sub>N collimator would normally be used with this cell on a focused monochromatic beam to reduce the extraneous scattering, but this is unnecessary in the nearly parallel beam on VIVALDI, and indeed would be disadvantageous due to the production of  $\gamma$ -rays near the image-plate detector.

The shadowing of the diffraction patterns by the Cd-clad pillars and the upper and lower anvil supports is obvious in figure 3. It is also apparent that the radial projection of reciprocal space rotates twice as fast as the shadow of the pillars, even though the cell and the sample rotate as one. Reflections obscured by the pillar at one value of  $\phi$  are visible  $20^\circ$  away in  $\phi$  at a different wavelength. This allows measurement of reflections that would be obscured completely in a monochromatic experiment. The background from the steel gasket, the principal source of background in the cell, has little structure, despite the volume of gasket irradiated being  $\sim 20 \text{ mm}^3$ .

On close inspection we can also identify three diffraction patterns, one from the nearly cubic natrolite sample, and two from the two tips of the conical moissanite anvils. Each pattern could be indexed, and in addition the displacements of the origin of each pattern with respect to

<sup>7</sup> The total path length in the beam is *twice* the wall thickness. The same applies to the cryostat heat shields and to the gasket of the anvil cell.



**Figure 3.** Two Laue diffraction patterns from a 0.5 mm<sup>3</sup> natrolite sample in a moissanite-anvil cell: (a)  $\phi = 65^\circ$ , exposure time 1 h; (b)  $\phi = 75^\circ$ , exposure time 1/2 h.

the ideal centre determined. In the real experiment, we would use patterns separated by about  $90^\circ$  in  $\phi$  to determine the translations of the cell both vertically and across the beam in two directions to centre the sample in the beam and then we would reduce the aperture diameter to bathe just the sample.

Five patterns at different values of  $\phi$  from  $-105^\circ$  to  $75^\circ$  were collected for a total exposure time of three hours. We integrated each of the diffraction patterns in the usual way, accepting just those reflections within the unshadowed region in each pattern. The reflections from the sample and each anvil were treated separately, since our integration algorithm uses the shapes of nearby strong reflections to define the integration limits for the weaker reflections (Wilkinson *et al* 1988). The sets of natrolite and moissanite reflections were each normalized to a common wavelength via the usual empirical procedure. The structure of natrolite was then refined by least squares against the normalized set of observations for natrolite to give the coordinates and thermal-displacement parameters listed in table 1. All coordinates agree within three estimated standard deviations (esds) with previously published neutron data (Torrie *et al* 1964, Pechar *et al* 1983). The esds on  $x$  and  $y$  are similar to, and at times smaller than, those of the earlier (monochromatic) data, but the esds on our  $z$  coordinates are typically an order of magnitude larger. This is undoubtedly due to the  $c$  axis being nearly perpendicular to the incident beam in all patterns, and also parallel to the axis of the pressure cell, which limits the extent of the data recorded with large values of  $l$ . This limitation would be partly relieved if the vertical access approached  $\pm 52^\circ$ , as has been achieved by Goncharenko and coworkers (Goncharenko 2004) in similar anvil cells. The large  $R$  factor is due to the large percentage of weak data that are accepted. The huge gain in data collection rate afforded by the Laue technique is evident when we note the data of Pechar *et al* were collected from a 12 mm<sup>3</sup> crystal over a period of more than 500 h, albeit at a low-flux reactor.

**Table 1.** Fractional atomic coordinates and isotropic thermal displacement parameters ( $\text{\AA}^2$ ) for natrolite,  $\text{Na}_2\text{Al}_2\text{Si}_3\text{O}_{10}\cdot 2\text{H}_2\text{O}$ , at 295 K in a moissanite-anvil pressure cell. Space group  $Fdd2$ ;  $a = 18.30 \text{ \AA}$ ,  $b = 18.63 \text{ \AA}$ ,  $c = 6.60 \text{ \AA}$ ; 1621 acceptable recorded reflections, 603 unique;  $R(F) = 0.15$ , Goodness-of-fit = 1.88. Standard deviations are given in parentheses.

	$x$	$y$	$z$	$U_{\text{iso}}$
Na	0.2215(5)	0.0312(5)	0.6083(56)	0.014(2)
Al	0.0377(4)	0.0952(4)	0.5991(54)	0.002(2)
Si(1)	0	0	0	0.010(2)
Si(2)	0.1532(4)	0.2117(4)	0.6113(45)	0.006(2)
O(1)	0.0227(3)	0.0684(3)	0.8540(51)	0.017(2)
O(2)	0.0699(2)	0.1821(3)	0.5957(50)	0.007(1)
O(3)	0.0983(4)	0.0347(3)	0.4882(47)	0.012(1)
O(4)	0.2064(4)	0.1532(3)	0.7222(51)	0.013(2)
O(5)	0.1810(3)	0.2272(4)	0.3765(56)	0.017(1)
O(6)	0.0573(4)	0.1888(4)	0.1131(50)	0.021(2)
H(1)	0.0535(9)	0.1462(9)	0.0478(70)	0.049(4)
H(2)	0.1049(10)	0.1868(9)	0.1677(72)	0.051(4)

**Table 2.** Fractional atomic coordinates and isotropic thermal displacement parameters ( $\text{\AA}^2$ ) for the moissanite anvils, (6H) SiC, at 295 K in a moissanite-anvil pressure cell. Space group  $P6_3mc$ ;  $a = 3.08 \text{ \AA}$ ,  $c = 15.12 \text{ \AA}$ ; 913 acceptable recorded reflections, 118 unique;  $R(F) = 0.20$ , Goodness-of-fit = 3.53.  $U_{\text{iso}}$  constrained to be the same for all atoms of the same species. Standard deviations are given in parentheses.

	$x$	$y$	$z$	$U_{\text{iso}}$
Si(1)	0	0	0	0.01(2)
Si(2)	2/3	1/3	0.1732(39)	0.01
Si(3)	1/3	2/3	0.3378(45)	0.01
C(1)	0	0	0.1338(29)	0.03(1)
C(2)	2/3	1/3	0.3009(42)	0.03
C(3)	1/3	2/3	0.4651(41)	0.03

Finally, to demonstrate that only a fraction of the sample need be bathed in the beam, we also refined the structure of moissanite against the combined sets of wavelength-normalized reflections from the two anvils. Table 2 lists the coordinates and thermal-displacement parameters which agree reasonably well with those reported by Gomes de Mesquita (1967). Again the esds on the  $z$  coordinates are large due to the nearly perpendicular alignment of the  $c$  axes of both anvils to the incident beam. Both the  $R$  factor and the goodness-of-fit are large due to the very large extinction.

No correction for absorption was made in this study. The cylindrical geometry would facilitate calculation of a correction, although the cylindrical symmetry would be lost for a small crystal located off-axis in the anvil cell. Even in that case the determination via the orientation refinement of the centre of the sample with respect to the anvils, and thence the gasket, would permit reasonably precise calculation for each reflection individually of the absorption in the gasket (both incident and diffracted beams) and in the anvil traversed by the diffracted beam. This cell can be cooled in a He cryostat, and the pressure monitored using ruby fluorescence via an optical fibre, although at 51 mm the diameter of the cell is slightly too big for the dedicated VIVALDI cryostat (49 mm bore).

We note that the efficiency of the image plates used in this study was  $\sim 7\%$  at the mean wavelength. The present plates are  $\sim 20\%$  efficient, which would improve considerably the statistics for the same exposure times.



## 7. Conclusions

We have demonstrated that full crystallography in a pressure cell is quite feasible using the white-beam Laue technique, despite some disadvantages inherent to the Laue technique. Either opposed-piston or anvil cells can be used, although some attention must be paid during the construction of the cell to maximize the accessible solid angle and to reduce the amount of material in the incident and transmitted beams. With a pillared cell the Laue technique is better suited than the monochromatic technique in that the pillars do not definitely obscure some regions of reciprocal space. Pressure calibration cannot be done via lattice parameter measurement, but requires either direct measurement of the pressure or visual access to use ruby fluorescence. Our examination and demonstration of possible pressure cells are hardly exhaustive, but the general conclusions apply also to time-resolved Laue diffraction.

## Acknowledgments

We thank Chris Dobe and Philip Tregenna-Piggott of the University of Bern for allowing us to show their patterns from Cr ammonium Tutton's salt, and Philippe Decarpentrie and John Archer for expert technical assistance.

## References

- Bau R, Ho N N, Schneider J J, Mason S A and McIntyre G J 2004 *Inorg. Chem.* **43** 555–8
- Boss S R, Cole J M, Haigh R, Snaith R, Wheatley A E H, McIntyre G J and Raithby P R 2004 *Organometallics* **23** 4527–30
- Chung E, Lees M R, McIntyre G J, Balakrishnan G, Hague J P, Visser D, Paul D McK and Wilkinson C 2004 *J. Phys.: Condens. Matter* **16** 7837–52
- Cipriani F, Castagna J C, Wilkinson C, Oleinek P and Lehmann M S 1996 *J. Neutron Res.* **4** 79–85
- Dobe C, Noble C, Carver G, Tregenna-Piggott P L W, McIntyre G J, Barra A-L, Neels A, Janssen S and Juranyi F 2004 *J. Am. Chem. Soc.* **126** 16639–52
- Gobrecht K, Mélési L and McIntyre G J 1992 *ILL Internal Report* 92GO04T
- Gomes de Mesquita A H 1967 *Acta Crystallogr.* **23** 610–7
- Goncharenko I N 2004 *High Pressure Res.* **24** 193–204
- Helliwell J R, Habash J, Cruickshank D W J, Harding M M, Greenhough T J, Campbell J W, Clifton I J, Elder M, Machin P A, Papiz M Z and Zurek S 1989 *J. Appl. Crystallogr.* **22** 483–97
- Kernavanois N, Ressouche E, Laborier J-L, Mélési L and Thomas F 2004 *Physica B* **350** e873–5
- Mao H K, Xu J and Bell P M 1986 *J. Geophys. Res.* **91** 4673–6
- McWhan D B, Vettier C, Youngblood R and Shirane G 1979 *Phys. Rev. B* **20** 4612–23
- Pechar F, Schäfer W and Will G 1983 *Z. Kristallogr.* **164** 19–24
- Popov A I and McIntyre G J 2005 in preparation
- Schobinger-Papamantellos P, Wilkinson C, Ritter C, Tung L D, Buschow K H J and Moze O 2004 *J. Phys.: Condens. Matter* **16** 6569–78
- Torrie B H, Brown I D and Petch H E 1964 *Can. J. Phys.* **42** 229–40
- Wilkinson C, Cowan J A, Myles D A A, Cipriani F and McIntyre G J 2002 *Neutron News* **13** 37–41
- Wilkinson C, Khamis H W, Stansfield R F D and McIntyre G J 1988 *J. Appl. Crystallogr.* **21** 471–8
- Xu J, Mao H-K, Hemley R J and Hines E 2002 *J. Phys.: Condens. Matter* **14** 11543–8